Light-induced states of H and H^-, shadow states, and the dressed potential

A. S. Fearnside and R. M. Potvliege
Physics Department, University of Durham, Science Laboratories, Durham DH1 3LE, England

Robin Shakeshaft
Physics Department, University of Southern California, Los Angeles, California 90089-0484
(Received 8 August 1994)

Light-induced "bound" states of atoms originate from the movement of poles of the multichannel scattering matrix on the Riemann energy surface. The appearance of additional "bound" states of the negative hydrogen ion, recently predicted in the high-frequency theory, is related to the motion of resonance poles that correspond to autoionizing states in the absence of the field. Various pole trajectories leading to light-induced states are described for photodetachment from a one-dimensional square potential well. Certain light-induced states in atomic hydrogen are discussed in relation to the spectrum of the dressed Coulomb potential.

PACS number(s): 32.80.Rm, 03.80.+r

I. INTRODUCTION

The Floquet theory of multiphoton ionization of an atom by an intense laser field can be formulated in a frame of reference, often called the Kramers-Henneberger frame, which oscillates about the nucleus at the frequency of the field. The transformation to this frame simplifies the description of the atom appreciably when the frequency of the field is much higher than the characteristic frequencies of the unperturbed atom. Indeed, in the high-frequency limit the active electron(s) simply move in a time-independent "dressed" potential, which is just the static, cycle-averaged part of the interaction potential in the oscillating frame. In this "static" — or "high-frequency" — approximation the dressed bound states of the atom do not ionize, and their quasienergies are the real energies of the bound states supported by the dressed potential. The range of the dressed potential increases with the amplitude of the quiver motion of the electron. Therefore, as the intensity or the wavelength of the laser field increases, the number of bound states supported by the dressed potential may also increase, i.e., new bound states may appear, a phenomenon found by Bhatt, Piraux, and Burnett in their work on electron scattering from a polarization potential in the presence of strong monochromatic light [1–3]. The appearance of new bound states was later observed by several other investigators, e.g., by Bardsley and Comella [4] and Yao and Chu [5] in their study of photodetachment from a one-dimensional Gaussian potential. More recently, Muller and Gavrila [6] carried out fully correlated calculations on the structure of the negative hydrogen ion in the high-frequency limit, and also found such light-induced bound states.

In full Floquet calculations the nonstatic components of the Kramers-Henneberger potential are included, and their inclusion allows the atom to decay. Hence, the quasienergies of "bound" states, when calculated beyond the high-frequency approximation, are complex, and their imaginary parts are negative since the states decay. Bardsley and Comella, and also Yao and Chu, not only calculated the energy levels of the dressed Gaussian potential, but they also carried out full Floquet calculations of complex quasienergies for this system. They verified that the static approximation is indeed reliable at high frequency, both in giving accurate ac-Stark shifts of the dressed states and in correctly predicting the appearance of light-induced states. In the cases they studied, the appearance of a light-induced bound state of the dressed potential always coincided with the appearance of a light-induced state in the full Floquet calculation. Yet, light-induced states other than those obtained in high-frequency calculations are also possible; cases are known where a full Floquet calculation yields a light-induced state with no obvious counterpart in the spectrum of the dressed potential. For example, full Floquet calculations carried out for atomic hydrogen, for wavelengths in the vacuum ultraviolet (vuv) [7] as well as in the infrared or the visible [8,9], have revealed new discrete states, and yet the dressed Coulomb potential does not support additional bound states at high intensity. The appearance of light-induced states similar to those found in hydrogen has also been established for sodium and potassium [10]. Thus, while a new bound state supported by the dressed potential is a high-frequency limiting case of a light-induced time-decaying Floquet state, not all light-induced states correspond to new bound states supported by the dressed potential.

The purpose of this paper is to provide further clarification of the origin of light-induced states. (We use the term "light-induced state" to mean *any* new discrete state induced by a laser field, which may or may not correspond to a new bound state supported by the dressed potential. When we need to distinguish the new discrete states found in full Floquet calculations from those found in the high frequency theory we refer to the latter as "light-induced bound states supported by the dressed potential" or an equivalent circumlocution.) For the sake of clarity, we start with a brief description of

the analytic structure of the multichannel scattering matrix and of some general properties of the wave functions associated with light-induced states. These considerations are illustrated in Sec. III A by analyzing the appearance of a light-induced state in the one-dimensional (1D) Gaussian potential model of Cl^- studied by Yao and Chu. The relationship of light-induced states of negative ions to autoionizing states of the field-free system is discussed in Sec. III B, in a nonrigorous fashion; our earlier remarks about this problem [11] are amplified in view of the recent prediction of light-induced states in H^- [6]. Results for photodetachment from a one-dimensional square potential well are presented in Sec. III C for various wavelengths. Although the dressed Coulomb potential does not support new bound states at high intensity, light-induced states of atomic hydrogen do appear in intense high frequency fields [7], as noted above; in Sec. III D we show how the bound-state spectrum of the dressed Coulomb potential is related to these light-induced states. It should be noted that the existence of light-induced states has yet to be confirmed in experiment. All those light-induced states found so far in calculations for hydrogen and alkali-metal atoms have large ionization widths, which would make their detection difficult.

II. THEORY

A. Wave functions of light-induced states

Let us assume that the system consists simply of one active electron, initially bound by a short-range force, exposed to a monochromatic laser field. We make the dipole approximation and the Floquet ansatz (we assume that the intensity is constant) and we work in the $\boldsymbol{p}\cdot\boldsymbol{A}$ gauge. The wave function of any discrete dressed state of the system is a solution of the Schrödinger (Floquet) equation satisfying Siegert boundary conditions. Outside the range of the potential it reduces to a linear superposition of infinitely many spherical waves $\exp[ik_M(E)r]/r$ in three dimensions or plane waves $\exp[ik_M(E)|x|]$ in one dimension, where E is the (complex) quasienergy and $k_M(E)$ is a channel wave number; if ω is the photon angular frequency, we have

$$k_M(E) = [(2\mu/\hbar^2)(E + M\hbar\omega)]^{1/2}, \tag{1}$$

where μ is the mass of the electron. Hereafter, when there is no possibility of confusion, we abbreviate $k_M(E)$ as k_M. We denote by M_0 the smallest integer M such that $\mathrm{Re}(E) + M\hbar\omega > 0$. For each channel wave number, there are two different branches of the square root function, and the choice of branch determines whether or not the eigensolution describes a "dominant" state, i.e., a decaying bound state which is physically significant, or a nonphysical state. If the state is dominant, its quasienergy must have an imaginary part that is negative and, at asymptotically large distances, its wave function must behave as an outgoing wave in the open channels (i.e., channels $M \geq M_0$) and vanish in the closed channels ($M < M_0$). Therefore, the wave numbers must be such that $-\pi/4 < \arg(k_M) \leq 0$ for $M \geq M_0$ and $\pi/2 \leq \arg(k_M) < 3\pi/4$ for $M < M_0$; these are the "physical" branches. States whose wave functions do not satisfy these conditions may be either antibound states or "shadows" of dominant states or antibound states. Shadow states, which are discussed further in the next subsection, are analytic continuations, onto different sheets of the Riemann energy surface, of discrete states — either true bound states, physically significant resonances, or antibound states — of the bare system. A nondominant (i.e., shadow or antibound) state corresponds to the choice of an "unphysical" branch for at least one wave number. Dominant and shadow states are associated with dominant and shadow poles, respectively, of the multichannel scattering matrix [12]. Dominant poles lie close to the physical energy axis, while shadow poles lie relatively far from this axis. Dominant states can be defined in a mathematically rigorous way in the framework of the complex scaling method provided the potential is suitable. Shadow states are not uncovered by the usual complex scaling method, although in some cases they are amenable to numerical calculation (e.g., by using expansions on complex basis sets [11,13] or by using a modified version of the complex scaling method [14] or, for a finite range potential, by using the method described in the Appendix). The light-induced states are particular instances of dominant states.

The quasienergy and the wave function of a dominant state vary with the amplitude of the laser electric field, as well as with the frequency and the polarization, and at some intensity a multiphoton threshold may be crossed (i.e., M_0 changes by unity). However, it is advantageous to study these functions in a domain of definition larger than that where the state is dominant. Hence, we analytically continue the quasienergy and the wave function and consider that they vary continuously across the thresholds, without any jump in $\arg(k_{M_0})$. (It is also interesting, though not necessary for our purposes, to study their variation for complex values of the parameters of the field [15].) Dominant and shadow states are treated on the same footing in this way. Any dominant state becomes a shadow state upon passage by a multiphoton threshold. In particular, any light-induced state becomes a shadow state when the intensity decreases below its appearance intensity. (In all cases analyzed so far, for hydrogen, alkalies, and model systems alike, the light-induced states appear at an intensity where the real part of their quasienergy is an integral multiple of the photon energy, i.e., right at a multiphoton threshold; evidently, the binding energy of a light-induced bound state supported by the dressed potential is zero at its appearance intensity.)

The question of the zero-field limit of light-induced states has not received a great deal of attention so far. On general grounds, one would expect that all dominant and shadow states reduce to discrete states of the bare system in the zero-intensity limit, i.e., to bound or antibound states or field-free resonances. For example, it has been shown [13] that at least one of the light-induced states found by Bardsley, Szöke, and Comella [16] for

the one-dimensional Gaussian potential could indeed be traced back to a true excited bound state in this limit. However, we are not aware of any rigorous mathematical study of the zero-field limit of light-induced states.

B. Poles of the scattering matrix

The appearance of light-induced states can be discussed in terms of trajectories of poles of the multichannel scattering matrix. The scattering matrix has poles in the energy variable at those (quasi)energies where the system has discrete states. Furthermore, it has infinitely many branch points on the real axis, one at each multiphoton ionization threshold where one of the k_M vanishes, in addition to branch point(s) at thresholds of the bare system. We draw cuts from each branch point downwards in the lower-half energy plane, parallel to the imaginary axis, so that each sheet of the Riemann manifold corresponds to a different choice of branches of the square root functions in Eq. (1). This choice of cuts, while not new, departs from the usual convention of drawing the cuts overlapping on the real axis. In our case, the poles that are dominant at a given energy (those associated with dominant states) can be reached from the real axis of the physical sheet by a path starting at this energy and going downwards without crossing any cut. In other words, with our choice of cuts any dominant pole lies *on* the physical sheet. In general, the dominant poles are closer to the real physical axis than the other poles, and therefore have a greater influence on how the scattering amplitudes vary with energy; only near thresholds can shadow poles and antibound-state poles be of any physical significance.

In the absence of the radiation field, the multiphoton ionization channels are uncoupled and, therefore, the scattering matrix is single valued when it is continued along a closed path that encirles a multiphoton ionization branch point without encircling a branch point (threshold) of the bare system. Hence, when the radiation field is very weak, any pole that represents a bound state or resonance of a bare atomic system must have a shadow partner, at almost the same location, on each of those unphysical sheets that can be reached without encircling a threshold of the bare atomic system [12]. As the intensity increases, and the multiphoton ionization channels become more strongly coupled, these shadow poles may follow very different trajectories on the Riemann manifold, and some of them may move close to the physical energy axis and become physically significant. Often, the trajectories of these poles are such that when a dominant pole shifts across a cut and takes on a shadow character, it is replaced, at about the same intensity and at about the same energy, by a shadow pole which becomes dominant. Conversely, there are cases where a dominant pole shifts across a cut without being replaced by a dominant pole [17]. On the other hand, *a light-induced state appears when a shadow pole becomes dominant without replacing an existing dominant pole.* A light-induced state also appears when an antibound-state pole becomes dominant.

It should be noted that the quasienergy E of any dominant or shadow state has a multiplicity of values, differing from one another by an integral multiple of $\hbar\omega$, but associated with wave functions that differ from one another only by an overall phase factor. Thus, any discrete state of the system gives rise to infinitely many poles of the scattering matrix. These poles appear in different elements of the scattering matrix and correspond to laser-assisted resonances associated with the *same* state of the dressed target, i.e., they arise from stimulated absorption and emission of photons from and to the same state. A dominant pole and all of its multiples are located on the same (physical) sheet of the Riemann surface. However, a shadow pole and its multiples lie on different sheets, as we now explain. Suppose that a shadow pole is located at energy E, and that it corresponds to choosing the unphysical branch for the Mth wave number, i.e., $k_M(E)$. (Since the pole is a shadow pole, at least one of the wave numbers must take on the unphysical branch). To reach this shadow pole (from the physical sheet) the Mth branch cut must be crossed. Now consider a multiple of this shadow pole, located, say, at energy $E + L\hbar\omega$. This multiple corresponds to choosing the unphysical branch for $k_{M-L}(E + L\hbar\omega)$, and to reach this multiple the $(M - L)$th branch cut must be crossed, so it lies on a different sheet. Hence, a shadow pole and its multiples each lie on a different (unphysical) sheet. Let E_0 denote the energy of the field-free state to which a dressed state reduces in the zero-field limit; in this limit the different quasienergies corresponding to this dressed state reduce to $E_0 + n\hbar\omega$, with $n = 0, \pm1, \pm2, \ldots$. The numerical results described in the following are normalized so that $n = 0$, except where stated otherwise.

The role of shadow poles in multiphoton processes was first addressed by Ostrovskii [2], and we refer the interested reader to a fairly detailed discussion of the theory given several years ago by Shakeshaft and co-workers [11,15].

III. RESULTS AND DISCUSSION

A. One-dimensional model of Cl$^-$

Yao and Chu [5] studied the quasienergies of a one-dimensional model of the negative chlorine ion irradiated by an intense monochromatic electric field $F(t) = F_0 \cos\omega t$, at the wavelength (193 nm) of the ArF excimer laser. Their potential,

$$W(x) = -W_0 e^{-(x/x_0)^2}, \tag{2}$$

has the same form, but different strength and range, than that of Bardsley and co-workers [4,16]. Yao and Chu took $W_0 = 0.27035$ a.u. and $x_0 = 2$ a.u. In the absence of the field this potential supports only one bound state, with a binding energy of 3.6 eV. The first light-induced state appears at a field strength $F_{\rm app}$ of about 0.061 a.u. We have extended the calculations of Yao and Chu to field strengths below $F_{\rm app}$ using the same method as that used in Ref. [13] to study a similar case. Namely,

our calculations were performed on a double discrete basis set composed of short-range L^2 functions (these were harmonic oscillator eigenfunctions) and continuum functions $\exp(ik_M|x|)\,\Theta(x)$ satisfying the appropriate boundary conditions; the cutoff function $\Theta(x)$ is zero at $x = 0$, is small for x within the range of the potential, and is unity for x outside the range of the potential [18].

In Fig. 1 we show the trajectory in the complex energy plane, as the field strength F_0 varies, of the pole of the scattering matrix corresponding to the quasienergy E of this light-induced state. When $F_0 > F_{\rm app}$ we have $\pi < \arg(E) < 3\pi/2$; the real part of E is negative, as befits a bound state, but the imaginary part is nonzero, and negative, since this bound state decays through the absorption of one photon ($\hbar\omega = 6.4$ eV). The Floquet wave function describing the new bound state has a closed-channel component, representing the bound electron, and an open-channel component representing the free electron that has absorbed a photon. The closed-channel component satisfies the usual boundary condition of a bound state, namely, it decreases exponentially at large distances as $\exp(ik_0|x|)$ where $k_0 = [(2\mu/\hbar^2)E]^{1/2}$ with $\pi/2 < \arg(k_0) < 3\pi/4$. The open-channel component satisfies the usual exploding *outgoing-wave* boundary condition of a physically significant resonance, that is, it behaves as $\exp(ik_1x)$ where $k_1 = [(2\mu/\hbar^2)(E+\hbar\omega)]^{1/2}$ with $-\pi/2 < \arg(E+\hbar\omega) < 0$ and $-\pi/4 < \arg(k_1) < 0$. The electron moves *outwards* from the potential as the bound state decays, so $\mathrm{Re}(k_1) > 0$. Let us follow the trajectory of the pole as F_0 decreases below $F_{\rm app}$, to $F_0 = 0$ (it is represented by a dotted line where $F_0 < F_{\rm app}$ and by a solid line where $F_0 > F_{\rm app}$); $\arg(E)$ increases monotonically along this trajectory. When F_0 falls below $F_{\rm app}$, E crosses the negative imaginary axis and its real part becomes positive: M_0 decreases from 1 to 0. However, the state cannot decay by absorbing net zero photons. Indeed, as $\arg(E)$ increases past $3\pi/2$, $\arg(k_0)$ increases past $3\pi/4$, and since $\mathrm{Re}(k_0)$ remains negative $\exp(ik_0|x|)$ is still an *ingoing* (exponentially damped) wave, and so does not have the *outgoing* wave behavior expected of an open-channel component. The state has become a shadow state, with unphysical properties. When the quasienergy crosses the positive energy axis, so $\arg(E) > 2\pi$, the zero-photon open-channel component becomes an exploding ingoing wave [19]. As F_0 decreases still further, we see that the pole circles about the origin and finally, at $F_0 = 0$, it is on the negative real axis of the unphysical sheet [$\arg(E) = 3\pi$], at $|E| = 0.004246$ a.u. At this point, the shadow state is an *antibound* state of the bare system [20].

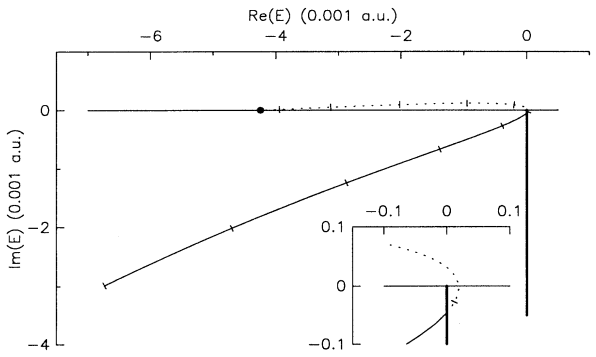

FIG. 1. The trajectory of the pole which, at field strengths above the appearance field strength $F_{\rm app}$, corresponds to the first excited bound state in the Gaussian potential studied by Yao and Chu [5]. The wavelength is 193 nm. The trajectory is represented by a dotted line where the pole is not dominant. The ticks on the trajectory are at intervals of 10^{-2} a.u. in F_0, and the zero-field position of the pole is marked with a solid circle. The thick vertical line represents the cut originating from the branch point at $E = 0$. The inset is a magnification of the region around this branch point.

A similar analysis was carried out for the new bound state of the dressed Gaussian potential that corresponds to the light-induced state that we just discussed. The dressed potential is

$$W_{\rm dr}(x) = \frac{\omega}{2\pi}\int_0^{2\pi/\omega} W(x+\alpha_0\cos\omega t)\,dt = W(x)\sum_{n=0}^{\infty}\left(\frac{\alpha_0}{x_0}\right)^{2n}\frac{H_{2n}(x/x_0)}{2^{2n}(n!)^2}, \tag{3}$$

where α_0 is the quiver amplitude, defined as $\alpha_0 = eF_0/(\mu\omega^2)$ with e the electron charge. Let $E_{\rm st}$ be the energy of the electron in this static (high-frequency) approximation; $E_{\rm st}$ is the counterpart of the quasienergy E of Fig. 1. We write $E_{\rm st} = \hbar^2k^2/2\mu$, with k pure imaginary when $E_{\rm st} < 0$. When the electron is outside the range of $W_{\rm dr}(x)$, its wave function is a superposition of free waves,

$$\psi(x) = ae^{-|kx|} + be^{|kx|}. \tag{4}$$

The state is an antibound state at those (negative) values of $E_{\rm st}$ where $a = 0$ and a true bound state at those values where $b = 0$. It is straightforward to integrate the Schrödinger equation numerically, as long as the range of $W_{\rm dr}(x)$ is not much larger than $1/|k|$. As is shown in Fig. 2, $E_{\rm st}$ is zero for $F_0 \approx 0.08$ a.u. $\approx F_{\rm app}$, below which field strength the state is an antibound state. Both $E_{\rm st}$ and $\mathrm{Re}(E)$ have the same zero intensity limit and remain close (in absolute magnitude) at any intensity.

B. Autoionizing states

A schematic diagram of the trajectory of the pole studied in Sec. III A is shown in Fig. 3(a). We have indicated one of the multiphoton ionization channel thresholds, namely, the one corresponding to the absorption of 0 photons. The pole is dominant along the solid line part of the trajectory and corresponds to a shadow state with unphysical character along the dotted line part. The pole begins as an antibound-state pole, situated on the negative real energy axis of an unphysical sheet of the Riemann surface, but at a sufficiently high intensity it crosses the branch cut emanating from the zero-photon threshold, and moves onto the physical sheet where it corresponds to a light-induced state.

In Fig. 3(b) we present a schematic diagram of a pos-

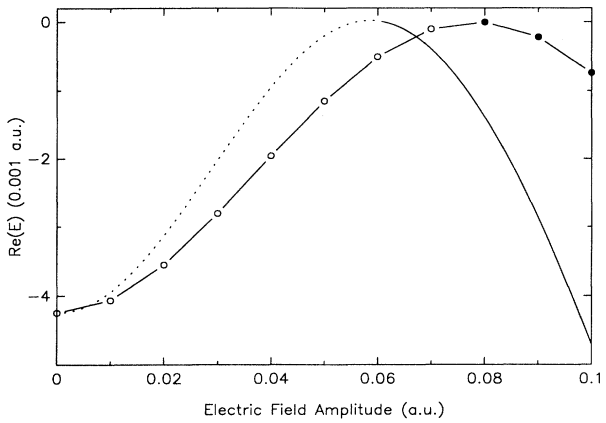

FIG. 2. The real part of the quasienergy of the same state as in Fig. 1 vs the electric field amplitude F_0. The curve is dotted where the state is not dominant. The circles indicate the energy E_{st} of the lowest light-induced bound state supported by the dressed potential (3) for a few values of F_0; the circles are open where the state is antibound.

sible trajectory of a pole which starts out corresponding to an autoionizing state. Initially the pole is on the physical sheet not far from the physical energy axis [$-\pi/2 < \arg(E) < 0$, $M_0 = 0$] so it is physically significant. At zero field strength the autoionizing-state wave function behaves at large distances as $\exp(ik_0 r)/r$ with $-\pi/4 < \arg(k_0) < 0$, that is, the wave function satisfies an exploding outgoing-wave boundary condition. At first, as the field strength increases, the autoionizing state becomes broader and shifts; the pole begins to move further away from the physical energy axis. Once the pole crosses the negative imaginary axis we have $-\pi < \arg(E) < -\pi/2$, whence $-\pi/2 < \arg(k_0) < -\pi/4$ although $M_0 > 0$; the pole takes on a shadow character. However, as the field strength increases further the pole crosses the same branch cut a second time, without crossing any other cuts. After this second crossing, $M_0 = 1$, $-3\pi < \arg(E) < -5\pi/2$ and $-3\pi/2 < \arg(k_0) < -5\pi/4$ — or, equivalently, since the branch point at $k_0 = 0$ is a square-root type (first order) branch point, $\pi/2 < \arg(k_0) < 3\pi/4$. The pole is now, once again, dominant,

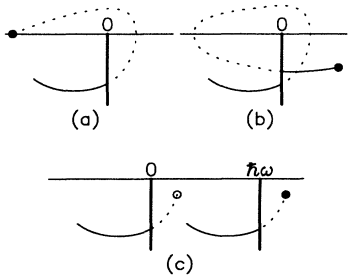

FIG. 3. Schematic diagram of a possible path of a pole which represents a state that begins at the solid circle (a) as an antibound state, or (b),(c) as an autoionizing state. As in Fig. 1, the trajectory is represented by a dotted line where the pole is not dominant.

and, since $\mathrm{Re}(E) < 0$, it corresponds to a light-induced bound state.

In a very weak field the dressed autoionizing state gives rise to infinitely many poles. In particular there are shadow poles located at (almost) the same energy, in the half plane $\mathrm{Re}(E) > 0$, as the field-free autoionizing pole; but these shadow poles are only on sheets that can be reached from the physical sheet by crossing the branch cut at the $M = 0$ threshold an even number of times, since this threshold is a threshold of the bare system. Hence, among the shadow poles which in a weak field are located at (almost) the same energy as the field-free autoionizing pole, none can emerge on the physical sheet in the half plane $\mathrm{Re}(E) < 0$, as F_0 varies, unless they encircle the $M = 0$ branch point an odd number of times. It is also impossible for one of these poles to move around the $M = 0$ branch point without crossing the cut at all (i.e., by moving onto the upper half plane on the physical sheet) since any pole lying on the physical sheet must have a negative (or zero) imaginary part.

On the other hand, suppose that the bare system has an autoionizing state with an energy whose real part is larger than $\hbar\omega$, so that in a weak field there is a shadow pole which is located to the right of the branch point at $\hbar\omega$. If, as the field varies, this shadow pole becomes dominant, it will, in general, be accompanied by the appearance of a dominant pole with $\mathrm{Re}(E) < 0$, since the multiples of a dominant pole all lie on the same (physical) sheet. This is illustrated in Fig. 3(c). In this diagram a shadow pole associated with the autoionizing pole shifts past the $M = -1$ branch point (at $\hbar\omega$) and becomes dominant. If E is the energy of this pole, another (multiple) pole is located at $E - \hbar\omega$, but before the poles become dominant they are on different sheets. The two poles become dominant, and move onto the physical sheet, simultaneously; the multiple appears on the physical sheet after passing the $M = 0$ threshold. When the poles are dominant, they correspond to a state that can be described as an autoionizing state dressed by the field, or, if the wave function is more similar to that of a dressed bound state, as a light-induced state. Therefore, an autoionizing state may change adiabatically into a light-induced state as the intensity increases, without ever disappearing as a physically realizable state of the system, provided its energy does not shift below the ionization threshold.

C. The 1D square potential well

The calculations presented in Sec. III A for the one-dimensional Gaussian potential well (2) were performed on a basis set, which somewhat limited their scope. We now turn to the case of photodetachment of an electron from the one-dimensional square potential

$$W(x) = \begin{cases} -W_0, & |x| \le a \\ 0, & |x| > a \end{cases} \qquad (5)$$

which can be tackled by using the more powerful method described in the Appendix. In the absence of the

field, the number of bound states supported by this well depends solely on the dimensionless parameter $\gamma = a(2\mu W_0/\hbar^2)^{1/2}$. We choose $a = 2.129619$ a.u. and $W_0 = 0.110247$ a.u. (3 eV). For these parameters, $\gamma = 1.000\,001$, there is only one bound state (with a binding energy of 0.05 a.u.) and the energy of the highest lying antibound state is -0.110 246 a.u. [21]. The trajectories of the bound-state pole, of some of its shadow poles, and of the antibound-state pole are presented in Figs. 4 and 5, for wavelengths between 266 nm ($\omega = 0.173$ a.u.) and 2128 nm ($\omega = 0.0214$ a.u.). (Because of their scale, the diagrams may suggest, incorrectly, that the slopes of some of the trajectories are not continuous. In fact, the positions of these poles vary smoothly with the intensity.) The real parts of the quasienergy of these states are compared to the energy levels that the electron can occupy in the high-frequency approximation in Fig. 6. The first light-induced bound state supported by the dressed square potential appears at $\alpha_0 \approx 4$ a.u.; the second one, not shown in Fig. 6, appears at $\alpha_0 \approx 20$ a.u.

The results of Figs. 4(a) and 5(a), for 266 nm wavelength, are typical of the high-frequency case. The trajectory of the antibound state pole is similar to that displayed in Fig. 1 for the Gaussian potential. The trajectory of the bound-state pole is also similar to that of the ground-state pole of atomic hydrogen in a high-frequency field [7]: The binding energy of the state decreases as the intensity increases, while the rate of multiphoton ionization, $-2\mathrm{Im}(E)/\hbar$, first increases and then decreases in the stabilization regime. (The rate increases again at very high intensity [22].) The antibound-state pole emerges on the physical sheet at an intensity very close to the appearance intensity of the first new bound state supported by the dressed potential [see Fig. 6(b)]. At higher intensity, the real part of the quasienergy of the light-induced state, as found in the full Floquet calculation, remains close to the energy of that new bound state. The ionization width of the light-induced state is large at the appearance intensity (about 0.004 a.u.). However, it decreases rapidly at higher intensity.

Results for 532 nm are presented in Figs. 4(b), 5(b), and 6. Overall, they are similar to those for 266 nm. The high-frequency approximation is not as good, though, but it improves at high intensity. The photoionization width of the light-induced state at its appearance intensity (1.59×10^{13} W/cm^2) is rather small, about 6.6×10^{-5} a.u., at this particular wavelength.

Photodetachment from the ground state in a weak field requires the absorption of at least two photons, at 1064 nm (i.e. $M_0 = 2$). In contrast with the previous cases, the energy shift of the ground-state pole is now negative. The dominant pole starting as the ground-state pole in zero field passes the two-photon threshold at 9.3×10^{12}

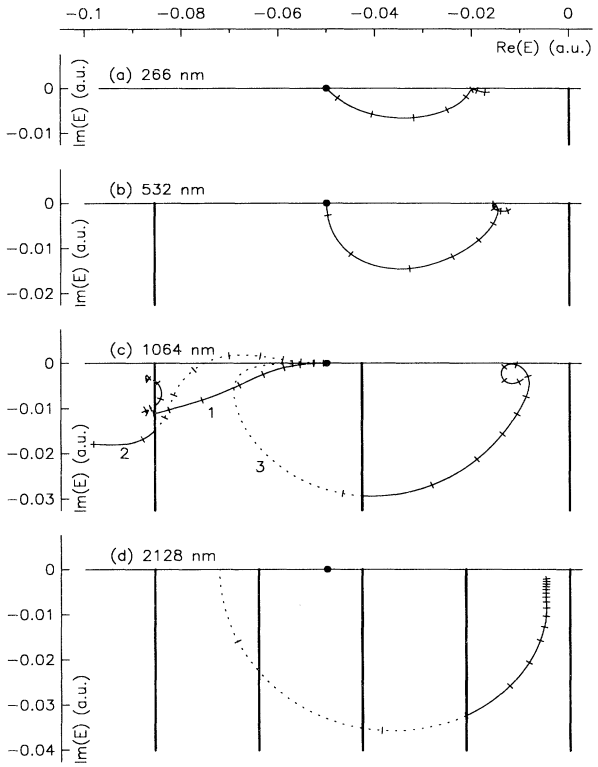

FIG. 4. Trajectory of poles that coincide with the bound-state pole of the square well potential (5) in the zero-field limit, for different wavelengths. The trajectory is represented by a dotted line where the pole is not dominant. The horizontal and vertical scales give Re(E) and Im(E), respectively, in a.u. The ticks on the trajectory are at intervals of 1 a.u. in α_0, and the zero-field position of the pole is marked with a solid circle. The thick vertical lines represent the cuts originating from the multiphoton branch points.

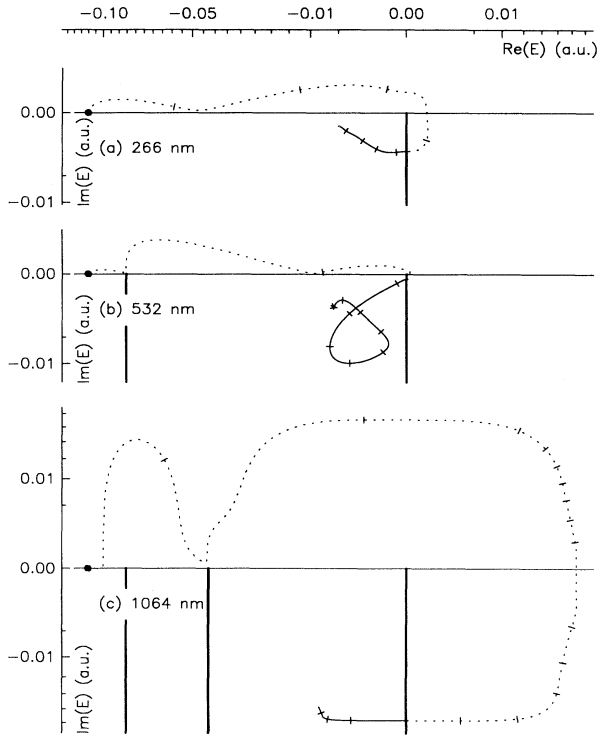

FIG. 5. The same as in Fig. 4, but for poles that coincide with the first antibound-state pole of the square well potential (5) in the zero-field limit.

W/cm^2; this pole is labeled 1 in Fig. 4(c). At 1.1×10^{13} W/cm^2, pole 2 also crosses the cut emanating from the two-photon threshold, upon which it becomes dominant and "replaces" pole 1 as the dominant ground-state pole. The trajectory of pole 1 brings it on the right of the two-photon threshold between 2.1×10^{13} and 2.8×10^{13} W/cm^2; it corresponds to a light-induced state in this interval of intensity, albeit one that does not appear to be related to any light-induced bound state supported by the dressed potential. Like pole 2, pole 3 starts in weak field as a shadow of pole 1. Yet, unlike pole 2, its shift soon changes sign and above 1.7×10^{11} W/cm^2 its trajectory is similar to that of the dominant ground state pole at 266 nm and 532 nm, although it lies on an unphysical sheet. Pole 3 becomes dominant at 5.55×10^{11} W/cm^2, and continues to follow a trajectory close to the trajectory the $1s$ dominant pole follows at higher frequency. In particular, the real part of the quasienergy of this state remains close to the energy of the ground state of the dressed potential—see Fig. 6(a)—and gets closer at high intensity.

The appearance at 1064 nm of a light-induced state associated with a shifted antibound state pole is illustrated in Figs. 5(c) and 6(b). The state appears at an intensity, about 2.45×10^{13} W/cm^2, 13 times higher than that calculated in the high-frequency approximation, and its photoionization width (0.058 a.u.) is very large at this intensity. However, this light-induced state is not a counterpart of the lowest light-induced bound state predicted by the high frequency theory. Instead, another light-induced state can be obtained at 1064 nm from that at 532 nm, by varying the intensity and the wavelength continuously starting at a large intensity. This other state is studied in Fig. 7. The pole it is associated with reduces, in the zero field limit, to a resonance pole shifted by $\hbar\omega$ (recall that the possibility that a light-induced state may originate in that way was suggested in Sec. IIB). Here we see that the state appears and disappears several times as the intensity increases. It first appears at a weak intensity, about 1.2×10^{11} W/cm^2, but with an extremely large width. The width decreases rapidly at higher intensity; at an intensity of 2.66×10^{13} W/cm^2, where $\alpha_0 = 15$ a.u., it is down to 8.7×10^{-3} a.u. and the real part is in good agreement with the binding energy of the lowest light-induced bound state supported by the dressed potential.

Finally, Fig. 4(d) illustrates a low frequency case: $M_0 = 3$ at the wavelength of the figure, 2128 nm. This case is similar, qualitatively, to the 1064 nm case. Here, a shadow pole of the bound-state pole starts by following closely the real axis, as the intensity increases from 0 to 5.845×10^9 W/cm^2, at which point the pole interacts with another pole — not shown in Fig. 4(d) — and it starts moving rapidly downward. The pole then describes a loop in the lower half plane, passes across three cuts, and emerges on the physical sheet at 6.64×10^{10} W/cm^2. Although the photon energy is quite a bit smaller than the ground-state binding energy of the field-free system, the energy of the ground state of the dressed potential still gives, at sufficiently high intensity, a good approximation to the real part of the quasienergy of the light-induced state [see Fig. 6(a)]. The appearance of this light-induced state reminds us of one that we previously

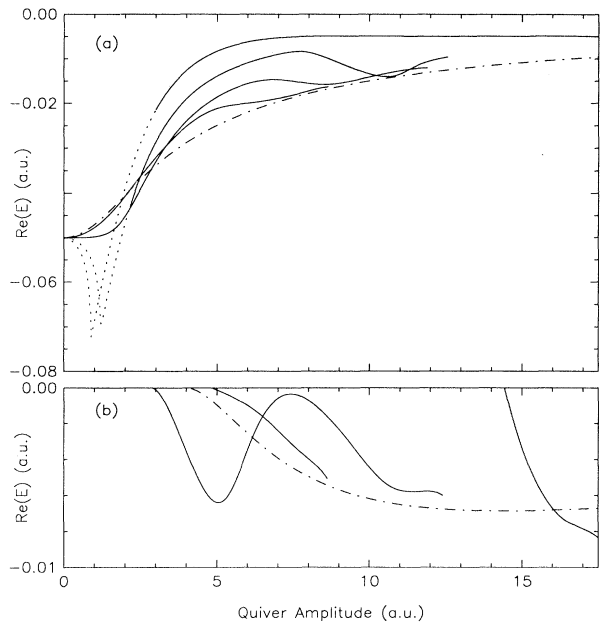

FIG. 6. (a) The real part of the quasienergy of the same states as in, Figs. 4(a), 4(b), and 4(d), and of state 3 of Fig. 4(c) vs the quiver amplitude α_0. The curve is dotted where the state is not dominant. The energy of the ground state of the dressed square potential is represented by a dash-dotted line. From top to bottom at $\alpha_0 = 5$ a.u., the curves correspond to the following wavelengths: 2128 nm, 1064 nm, 532 nm, 266 nm, and 0 nm (infinite frequency). (b) The same as in part (a), but for the same states as in Fig. 5. Here the dash-dotted line represents the energy of the lowest light-induced bound state supported by the dressed square potential. The curves starting from $\mathrm{Re}(E) = 0$ at $\alpha_0 \approx 3$, 5, and 14.5 a.u. correspond to 532 nm, 266 nm, and 1064 nm wavelength, respectively.

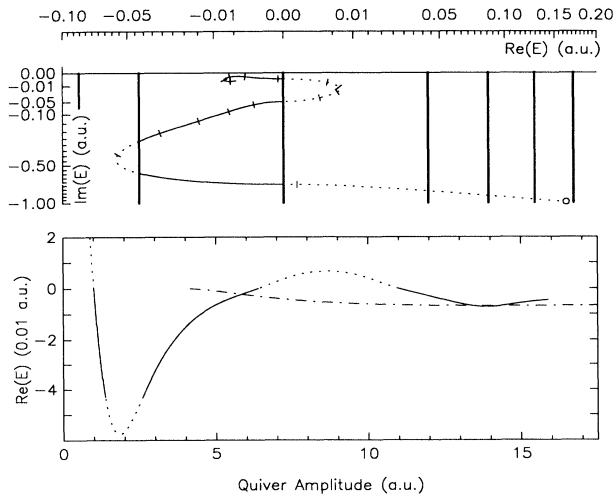

FIG. 7. The same as in Figs. 4 and 6, but for a pole which coincides in the zero-field limit with a resonance pole shifted to the left by $\hbar\omega$. The wavelength is 1064 nm.

described for multiphotoionization of atomic hydrogen in a low-frequency (infrared or optical) laser field [8,9]. Also worth noting in Fig. 6(a) is the closeness of the 1064 nm curve and the 2128 nm curve, which shows that α_0 remains a relevant dynamical parameter outside the high-frequency regime.

D. Light-induced states of H

The only discrete states of the bare hydrogen atom are bound states; atomic hydrogen has no resonance or antibound states, and so light-induced states can only evolve from shadows of bound states. In Fig. 8 we show the real part of the $1s$ quasienergy of atomic hydrogen *vs* the "quiver amplitude" α_0 for several different angular frequencies ω. The dash-dotted line is the quasienergy in the high-frequency limit, $|E_\infty|$ (i.e., the energy of the ground state of the dressed Coulomb potential) [23]. The other lines represent results of full Floquet calculations performed on a basis of complex Sturmian functions [7,24,25]. The broken lines pertain to frequencies larger than the threshold frequency, $\omega_{\rm thr} = 0.5$ a.u., for one-photon ionization from the $1s$ state in the weak-field limit, while the solid lines pertain to frequencies smaller than $\omega_{\rm thr}$. There is a striking similarity between these results and those shown in Fig. 6(a) for photodetachment from a one-dimensional square potential well.

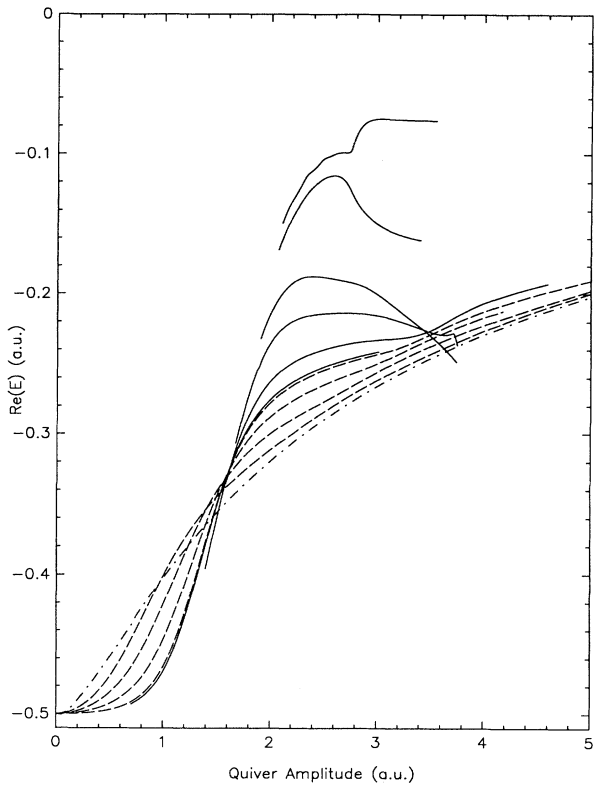

FIG. 8. The energy of the $1s$ state for $\omega = \infty$ (dash-dotted line), the real part of the quasienergy of the dressed $1s$ state for $\omega > 0.5$ a.u. (broken lines), and that of the the $1s'$ state for $\omega < 0.5$ a.u. (solid lines), vs the quiver amplitude α_0. From top to bottom, at $\alpha_0 = 2.5$ a.u., the curves correspond to the following frequencies: $\omega = 0.16$, 0.1713, 0.25, 0.30, 0.40, 0.49, 0.51, 0.65, 1.0, 2.0 a.u. and $\omega = \infty$.

When $\omega > \omega_{\rm thr}$ the binding energy can be calculated fairly accurately from the dressed Coulomb potential, even when $\omega \approx \omega_{\rm thr}$ [7]. Indeed, we see that the broken lines remain reasonably close to the dash-dotted line for all intensities, and approach it in the high-intensity and high-frequency limits. The energy of the dominant state which starts as the bare $1s$ state *increases* as the intensity increases, when $\omega > \omega_{\rm thr}$, while when $\omega < \omega_{\rm thr}$ the energy of this state *decreases* as the intensity increases (unless the dressed $1s$ state shifts into resonance with another state). On the other hand, when $\omega < \omega_{\rm thr}$ some of the shadow poles of the $1s$ pole — or, for that matter, any bound-state pole for which $M_0 > 1$ in a weak field — can move upwards in energy and become dominant, like pole 3 in Fig. 4(c). This is borne out by Fig. 8: the solid lines begin abruptly at a nonzero intensity and correspond to a light-induced state from which one-photon ionization is possible. The Sturmian basis is unsuitable for following the trajectory of the corresponding pole as it moves beyond the threshold for one-photon ionization when the intensity decreases below the appearance intensity. Consequently, we have not determined the zero-field limit of this state for the different values of the frequency. It most likely converges towards the $1s$ state when ω is not much smaller than 0.5 a.u.; but when $\omega \ll 0.5$ a.u. it is possible that it reduces to another bound state after having undergone an avoided crossing on an unphysical sheet. Since this light-induced state behaves in much the same way for $\omega \lesssim 0.5$ a.u. as the dressed $1s$ state behaves for $\omega \gtrsim 0.5$ a.u. we refer to it as a $1s'$ state. In principle, its binding energy is defined only modulo $\hbar\omega$, as is the case for any dressed state; this ambiguity was resolved, and all the results of Fig. 8 have been put on the same absolute scale, by making sure that the quasienergy varied continuously across and along the curves, in both intensity and in frequency.

The width of the $1s'$ state is very large at its appearance intensity. For example, at $\alpha_0 = 2.5$ a.u., its width is 7.8 eV for $\omega = 0.160$ a.u., 3.8 eV for $\omega = 0.30$ a.u., and 2.3 eV for $\omega = 0.49$ a.u. Nevertheless, its binding energy remains close to $|E_\infty|$ when $\omega \approx \omega_{\rm thr}$. There are significant differences when $\omega \ll \omega_{\rm thr}$, partly due to avoided crossings, in the range of intensity we have explored.

As a consequence of the smooth variation of the quasienergy with the intensity and the frequency, the binding energy of the $1s'$ state at its appearance intensity is a continuous function of the frequency. The variation of this function can be visualized by interpolating the points of origination of the solid curves in Fig. 8. The resulting curve remains below the dotted curve for $\omega > 0.35$ a.u., crosses it at $\omega \approx 0.35$ a.u., and increases rapidly above it for lower frequency. Since α_0 is proportional to the square root of the intensity, this means that the light-induced state appears at a significantly larger (lower) intensity when $\omega > (<) 0.35$ a.u. than that where $\hbar\omega = |E_\infty|$.

IV. CONCLUSIONS

It is now well established, for one-electron one-dimensional models, that the light-induced states found in the high-frequency approximation persist when the coupling with the field is fully taken into account. In this respect, calculations for simple models support Muller's and Gavrila's prediction of light-induced states in H$^-$ [6]. However, correlation is likely to play an important role in the negative ion, which evidently limits the scope of the comparison. As for the photodetachment rate, no firm conclusion can be drawn, either. It should be noted that in none of the model systems investigated so far are the widths of light-induced states narrow enough to make their appearance readily observable in an experiment (supposing for a moment that these systems were real).

It is possible to study the quasienergy and the wave function of a light-induced state at intensities below the appearance intensity by introducing shadow states whose wave functions satisfy unphysical boundary conditions. We argued in Sec. III B that the trajectory of the quasienergy in the complex plane, as the intensity decreases to zero, could be similar to that drawn in Fig. 3(a), or, when the light-induced state originates from an autoionizing state, to that drawn in Fig. 3(c) or Fig. 3(b). In fact, light-induced states other than those predicted by the high-frequency calculations of Muller and Gavrila may also occur in H$^-$. For example light-induced states originating from shadow states of the bound state of the bare system are possible. The results reported in Sec. III C also indicate that even low-frequency fields might produce light-induced states, at relatively modest intensities.

In Sec. III D we addressed the interpretation of the ground state of the dressed Coulomb potential for photon energies smaller than the binding energy of the bare $1s$ state, $|E_{1s}|$. It has been argued that the (intensity-dependent) ground-state energy of the dressed Coulomb potential, E_∞, should be in good agreement with the quasienergy of the dressed $1s$ state provided the intensity is so high that $|E_\infty| \ll \hbar\omega$. This proposition is indeed well supported by our results. In particular, there is still agreement when $\hbar\omega$ is slightly smaller than $|E_{1s}|$ — although the state whose quasienergy follows E_∞ is, in fact, a light-induced $1s'$ state in this case.

There is a remarkable similarity between the results described in Sec. III C for a one-dimensional finite-range potential and those described in Sec. III D for the three-dimensional Coulomb potential. Clearly, the appearance in full Floquet calculations of light-induced states associated with the energy levels of the dressed potential is a quite general feature at moderate and high intensities, over a wide range of frequencies.

ACKNOWLEDGEMENT

This work was supported by the National Science Foundation under Grant No. PHY9315704.

APPENDIX

The method for locating the dominant poles and the shadow poles of the S matrix for laser-assisted scattering by a one-dimensional square potential well is similar to the well known method for finding the energy levels in the field-free case. Namely, the wave function is written in Floquet form,

$$\Psi(x,t) = e^{-iEt/\hbar} \sum_{N=-\infty}^{\infty} e^{-iN\omega t}\psi_N(x), \tag{A1}$$

with $\Psi(x,t)$ obeying Siegert boundary conditions, and the quasienergy is determined by solving a system of transcendental equations expressing that the harmonic components $\psi_N(x)$ and their first order derivatives vary continuously at the edges of the well. Alternatively, scattering boundary conditions can be imposed if one wants to study laser-assisted scattering of electrons by the potential well [26].

The potential is given by Eq. (5). Piecewise continuous solutions of the Schrödinger equation

$$i\hbar\frac{d}{dt}\Psi(x,t) = \left[-\frac{\hbar^2}{2\mu}\frac{d^2}{dx^2} - i\hbar(e/\mu\omega)F_0\cos(\omega t)\frac{d}{dx} + W(x)\right]\Psi(x,t) \tag{A2}$$

can be written in the form of Volkov waves, e.g.,

$$A_\pm e^{-iEt/\hbar}e^{\pm ikx \mp ik\alpha_0 \sin\omega t} \tag{A3a}$$

for $|x| > a$, with $k = [2\mu E/\hbar]^{1/2}$, or

$$B_\pm e^{-iEt/\hbar}e^{\pm i\kappa x \mp ik\kappa\alpha_0 \sin\omega t} \tag{A3b}$$

for $|x| < a$, with $\kappa = [2\mu(E + W_0)/\hbar]^{1/2}$. As defined in Sec. III A, $\alpha_0 = eF_0/(\mu\omega^2)$. (We assume that $k \neq 0$ and $\kappa \neq 0$.) However, when $\alpha_0 \neq 0$ (and $W_0 \neq 0$) it is not possible to connect these solutions so as to construct a wave function that varies smoothly at $x = \pm a$ at all times, whatever the value of E. Infinitely many functions of the form (A3) must be superposed in order to obtain a suitable wave function $\Psi(x,t)$. Thus, we assert that $\psi_N(x)$ is given by

$$\sum_{M=-\infty}^{\infty} A_M J_{N-M}(-\alpha_0 k_M)e^{-ik_M x}, \tag{A4a}$$

for $x < -a$, with $k_M = [2\mu(E + M\hbar\omega)/\hbar]^{1/2} \neq 0$, by

$$\sum_{M=-\infty}^{\infty} B_M J_{N-M}(-\alpha_0\kappa_M)(e^{-i\kappa_M x} + (-1)^N e^{i\kappa_M x}), \tag{A4b}$$

for $|x| < a$, with $\kappa_M = [2\mu(E + W_0 + M\hbar\omega)/\hbar]^{1/2} \neq 0$, and by

$$\sum_{M=-\infty}^{\infty} (-1)^N A_M J_{N-M}(-\alpha_0 k_M) e^{ik_M x}, \qquad \text{(A4c)}$$

for $x > a$. The condition that each harmonic component is continuous and has a continuous first order derivative at $x = \pm a$ gives rise to a system of homogeneous linear equations relating the coefficients A_M and B_M to one another. The S matrix has poles at those values of E for which the system has a nontrivial solution.

In the present work, the indexes N and M were restricted to the same finite range, and the modulus of the (complex) eigenvalue of the matrix of the system nearest to zero was calculated as a function of E. The value of the modulus was less than 10^{-10} a.u., several orders of magnitude smaller than at the neighboring local minima, at the values of E we identified with dominant or shadow poles of the S matrix. When checked, this estimate of E could always be refined in order to bring the modulus down to zero to machine accuracy, without any significant change in the position of the pole.

[1] R. Bhatt, B. Piraux, and K. Burnett, Phys. Rev. A **37**, 98 (1988).

[2] The first discussion of light-induced states seems to be due to V. N. Ostrovskii, Teor. Mat. Fiz. **33**, 126 (1977) [Theor. Math. Phys. **33**, 923 (1977)], who studied the case of a particle moving in the one-dimensional potential $[a + b\cos(\omega t)]\delta(x)$ from a standpoint very similar to the one adopted here.

[3] An increase in the number of bound states supported by the dressed potential should not be expected to be a universal phenomenon, since the increase in range of the dressed potential is accompanied by a decrease in depth. However, one sees easily (by comparison with the field-free spectrum of square potential wells) that in one dimension the number of new bound states increases without limit, when the quiver amplitude increases, if the potential is short range and attractive everywhere.

[4] J. N. Bardsley and M. J. Comella, Phys. Rev. A **39**, 2252 (1989).

[5] G. Yao and S.-I Chu, Phys. Rev. A **45**, 6735 (1992).

[6] H. G. Muller and M. Gavrila, Phys. Rev. Lett. **71**, 1693 (1993).

[7] M. Dörr, R. M. Potvliege, D. Proulx, and R. Shakeshaft, Phys. Rev. A **43**, 3729 (1991).

[8] R. M. Potvliege and R. Shakeshaft, Phys. Rev. A **40**, 3061 (1989). The light-induced states are labeled 4 and 19 in Fig. 3 of this paper; their widths are about 0.04 eV and 0.2 eV, respectively, at their appearance intensity at 1064 nm.

[9] M. Dörr, R. M. Potvliege, and R. Shakeshaft, Phys. Rev. A **41**, 558 (1990). These light-induced states appear in Fig. 1 of this paper immediately on the right of the curves labeled 3p and 3d. The wavelength is 616 nm. The total rate of multiphoton ionization from the ground state is large, though without sharp enhancement, in the range of intensity where these light-induced states are in resonance with the dressed $1s$ state. Broad peaks in the photoelectron energy spectra measured by Rottke *et al.* at 608 nm are associated with this large ionization rate; However, the data cannot be interpreted as an unambiguous evidence of a light-induced state [H. Rottke, D. Feldmann, B. Wolff-Rottke, and K.H. Welge, J. Phys. B **26**, L15 (1993)].

[10] P. H. G. Smith (private communication). The calculations were performed on a one-electron model of these atoms.

[11] R. M. Potvliege and R. Shakeshaft, Phys. Rev. A **38**, 6190 (1988).

[12] R. J. Eden and J. R. Taylor, Phys. Rev. **133B**, 1575 (1964).

[13] M. Dörr and R. M. Potvliege, Phys. Rev. A **41**, 1472 (1990).

[14] A. Csótó, Phys. Rev. A **48**, 3390 (1993).

[15] M. Pont and R. Shakeshaft, Phys. Rev. A **43**, 3764 (1991).

[16] J. N. Bardsley, A. Szöke, and M. J. Comella, J. Phys. B **21**, 3899 (1988).

[17] This happens, e.g., for photodetachment from the Gaussian potential, in the case studied in Refs. [13,16], and for a particle in a time-periodic Rosen-Morse potential well [N. Moiseyev and H. Jürgen Korsch, Phys. Rev. A **44**, 7797 (1991)].

[18] Typically, the basis set included 31 L^2 functions of the form $\exp(-\alpha^2 x^2/2) H_n(\alpha x)$ with $\alpha = 1$ a.u. and 11 channel functions with $-5 \leq M \leq 5$ cut off smoothly at $x \approx 1.5$ a.u.

[19] Note that $\arg(k_M) > 0$ for all $M \neq 0$ in this range of field strength, with $\arg(k_0) < 0$. In fact, the quasienergy could not acquire a strictly positive imaginary part if the wave function was exponentially decreasing in *all* channels, for the wave function would then be square integrable for $\mathrm{Im}(E) > 0$, which is impossible, since square integrability implies that $\mathrm{Im}(E) = 0$. That is, no pole of the scattering matrix can lie on the upper half-plane of the *physical* energy sheet.

[20] A similar trajectory, ending with an antibound state, was also found by Ostrovskii, for the time-periodic δ potential. See Ref. [2] above.

[21] In the absence of the field, the energy of the antibound state E_{ab} is above (below) the bottom of the well, $-W_0$, when γ is larger (smaller) than 1. Here E_{ab} is just above $-W_0$. There is an antibound state with $E_{\mathrm{ab}} = -W_0$ when γ is exactly 1. However, its wave function cannot be written in the form of Eq. (A4b) with $N = M = 0$ since $\kappa_0 = 0$.

[22] A nonmonotonic decrease of the ionization rate at high intensity was also found by Yao and Chu [5] for the one-dimensional Gaussian potential, and by T. Millack [J. Phys. B **26**, 4777 (1993)] for the one-dimensional soft-Coulomb potential.

[23] The dash-dotted line in Fig. 8 is based on the results of M. Pont, N. Walet, and M. Gavrila [Phys. Rev. A **41**, 477 (1990)] for $\alpha_0 \geq 1.0$ a.u. and on those of C. K. Choi, W. C. Henneberger, and F. C. Sanders [Phys. Rev. A **9**,

1895 (1974)] for $\alpha_0 < 1.0$ a.u.

[24] See, e.g., the Appendix of the review paper by the present authors published in *Atoms in Intense Laser Fields* (Adv. At. Mol. Phys. Suppl. 1), edited by M. Gavrila (Academic, Boston, 1992), p. 373, for a description of the numerical techniques that were used. Typically, for $\omega = 0.4$ a.u. the basis set included 30 radial Sturmian functions for each partial wave ($0 \leq \ell \leq 5$) and harmonic component ($-4 \leq N \leq 6$) with $\arg(\kappa) = \pi/4$ and $|\hbar\kappa|^2/2\mu = 0.3$ a.u. in the notation of that paper.

[25] S.-I. Chu and J. Cooper, Phys. Rev. A **32**, 2769 (1985), had obtained a few points of the curve for $\omega = 0.49$ a.u.

[26] R. A. Sacks and A. Szöke, Phys. Rev. A **40**, 5614 (1989); S. Varró and F. Ehlotzky, J. Opt. Soc. Am. B **7**, 537 (1990); J. Z. Kamiński, Z. Phys. D **16**, 153 (1990). The scattering problem and the photodetachment problem have been studied by direct numerical solution of the time-dependent Schrödinger equation, too — see L. A. Collins and A. L. Merts, Phys. Rev. A **37**, 2415 (1988) and L. A. Bloomfield, J. Opt. Soc. Am. B **7**, 472 (1990).